Conformational Features of Tau Fibrils from Alzheimer's Disease Brain Are Faithfully Propagated by Unmodified Recombinant Protein

Olga A. Morozova, Zachary M. March, Anne S. Robinson, and David W. Colby*

Department of Chemical and Biomolecular Engineering, University of Delaware, Newark, Delaware 19716, United States

S *Supporting Information*

Human Alzheimer's disease brain-isolated tau PHFs + Recombinant tau → Fibrillization with conformational propagation
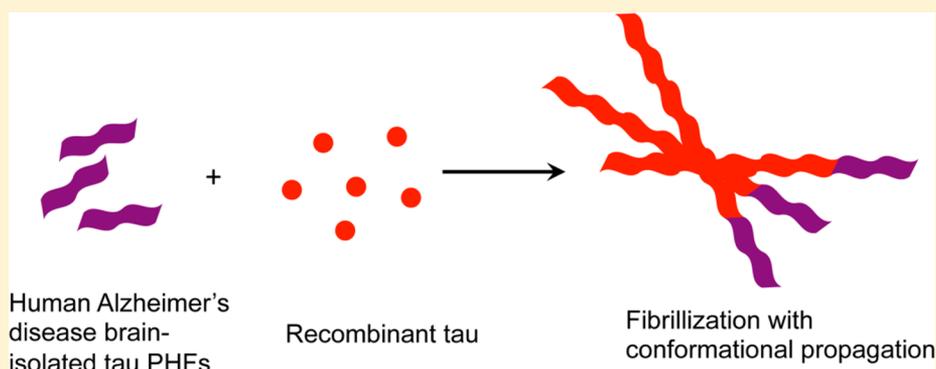
ABSTRACT: Fibrils composed of tau protein are a pathological hallmark of several neurodegenerative disorders including Alzheimer's disease (AD). Here we show that when recombinant tau protein is seeded with paired helical filaments (PHFs) isolated from AD brain, the amyloid formed shares many of the structural features of AD PHFs. In contrast, tau amyloids formed with heparin as an inducing agent—a common biochemical model of tau misfolding—are structurally distinct from brain-derived PHFs. Using ultrastructural analysis by electron microscopy, circular dichroism, and chemical denaturation, we found that AD seeded recombinant tau fibrils were not significantly different than tau fibrils isolated from AD brain tissue. Tau fibrils produced by incubating recombinant tau with heparin had significantly narrower fibrils with a longer periodicity, higher chemical stability, and distinct secondary structure compared to AD PHFs. The addition of heparin to the reaction of recombinant tau and AD PHFs also corrupted the templating process, resulting in a mixture of fibril conformations. Our results suggest that AD-isolated PHFs act as a conformational template for the formation of recombinant tau fibrils. Therefore, the use of AD PHFs as seeds to stimulate recombinant tau amyloid formation produces synthetic tau fibers that closely resemble those associated with AD pathology and provides a biochemical model of tau misfolding that may be of improved utility for structural studies and drug screening. These results also demonstrate that post-translational modifications such as phosphorylation are not a prerequisite for the propagation of the tau fibril conformation found in AD.

Tau is a microtubule-associated protein that stabilizes the microtubule network within neurons. Under normal physiological conditions, tau is a highly soluble, natively unfolded protein.[1] However, in more than 20 sporadic and familial neurodegenerative disorders, including Alzheimer's disease (AD), tau misfolds and forms insoluble fibril structures.[2−4] The formation of tau fibrils is associated with the loss of normal microtubule-stabilizing function, axonal transport deficits, and cell death.[5]

PHFs are tau fibrils found in human AD brain that have a distinct conformation.[2,6] These fibrils are made up of hyperphosphorylated tau protein, a post-translational modification of tau associated with early stages of the disease that may be an initiating factor in AD pathology.[3,7] This post-translational modification could occur either before or after each molecule joins the PHF. Hyperphosphorylation of tau can induce it to misfold.[8,9] However, fibrils formed of unphosphorylated tau may become phosphorylated by GSK-3β following oxidative stress.[10]

In addition to hyperphosphorylation, polyanionic cofactors such as heparin have been used as inducers of *in vitro* tau fibrillization to study the kinetics of amyloid assembly and the structure of resulting amyloids.[11−14] However, a physiological role for heparin in the mechanism for tau fibril formation seems unlikely, given its extracellular location *in vivo*, and the extent to which heparin-induced fibrils mimic the AD PHFs is a subject of debate.[11,12,15]

Distinct recombinant tau fibril conformations have been generated *in vitro* by the introduction of polymorphisms in the protein sequence. Upon cross-seeding by addition of fibrils of a given sequence to monomeric recombinant tau protein of another sequence, the fibril conformation of the seed is propagated by a templating effect.[16] Similar phenomena have

been observed *in vitro* with the amyloid β (Aβ) peptide[17,18] and *in vivo* with mammalian[19−22] and yeast[23,24] prion strains. Tau fibrils added to cultured cells or inoculated into transgenic mice have also been shown to accelerate the formation of filaments composed of endogenous tau, implying that a prion-like propagation of misfolded tau may contribute to the pathogenesis of tauopathies.[25−29] Additionally, distinct α-synuclein[30] and tau[31] filament structures have been shown to induce tau inclusions with distinctive features in cell and animal models, respectively.

PHFs isolated from AD brain tissue nucleate recombinant tau (rec tau) fibril formation.[32,33] By seeding rec tau with AD brain-derived PHFs, we find that conformational features of PHFs are conserved in the amyloid formed by a templated seeding effect. Our results suggest an improved biochemical model of PHF propagation and demonstrate that aberrant phosphorylation is not necessary for tau monomers to become incorporated into fibrils.

■ MATERIALS AND METHODS

Production and Purification of Recombinant Tau Protein. Recombinant 0N4R tau (rec tau) protein, the most prevalent tau isoform found in AD PHFs,[34,35] was purified from NEB5α E. coli (New England BioLabs) that was transformed with an IPTG-inducible pET 11a vector encoding the human 0N4R tau isoform under the T7 promoter.[36] Briefly, bacteria were grown at 37 °C in 5 mL of LB, 100 mg/mL ampicillin culture for 12 h before inoculation into a 2 L culture. This was grown until the culture reached an OD of 0.6−0.8 and induced with 0.5 μM IPTG. The bacteria were induced for 3 h before harvesting the cells followed by cell lysis. After sonication in purification buffer BRB80 (80 mM PIPES buffer, 1 mM EGTA, 1 mM MgCl), the cell lysate was boiled for 15 min, followed by ion exchange chromatography with phosphocellulose resin, where pure rec tau was eluted in 0.3 M NaCl. The resulting concentration was measured by UV spectroscopy and purity was measured with densitometry (Figure S1). The purified protein was frozen in −80 °C until immediately before use. Monomeric recombinant tau protein showed characteristics of random coil structure with no signs of misfolding (Figure S2).

Preparation of Brain Homogenates. Human brain tissue samples were obtained from the Harvard Brain Tissue Resource Center and the University of Pennsylvania Center for Neurodegenerative Disease Research. These samples included tissue from the frontal cortex of AD patients and normal controls. We followed a previously published protocol for brain tissue homogenization.[37] To prepare 5% (w/v) brain homogenates, nine volumes of ice-cold homogenization buffer (10 mM Tris, 1 mM EDTA, 0.8 M NaCl, 10% sucrose, and 0.1% Triton X-100) supplemented with protease inhibitors (1 mM PMSF; protease inhibitor cocktail P8340, Sigma) were added to brain tissue in a 50 mL tube. Brain tissue was homogenized on ice by extrusion through progressively smaller needles (10 passages each through 16, 18, and 21 gauge needles). The homogenate was centrifuged at 1000 × g for 5 min at 4 °C. The supernatant (S1) was collected, and the pellet was rehomogenized in 9 volumes homogenization buffer and protease inhibitors by 10 passages through a 21 gauge needle. This homogenate was then recentrifuged at 1000 × g for 5 min at 4 °C, and the resulting supernatant was combined with S1, yielding a 5 wt % brain homogenate.

Partially pure misfolded tau fractions were prepared as previously described.[37,38] In brief, starting with 4 mL of 5%

brain homogenate in 1% (w/v) Sarkosyl and 0.2% (w/v) dithiothreitol, we incubated the solution at room temperature for 2.5 h with stirring. Multimeric tau species were sedimented by ultracentrifugation at 300 000 × g for 1.5 h at 4 °C. The pellet was washed in PBS, centrifuged at 300 000 × g for 1.5 h at 4 °C, and resuspended in 4 mL PBS by stirring overnight at room temperature and passing 5 times through a 27-gauge needle to break up any residual aggregates. The resulting solution was aliquoted and stored at −80 °C.

Pure misfolded tau was isolated as described,[37,38] with slight modification. To reduce the possibility of structural modification of tau fibrils during purification, the partially pure tau fraction was not sonicated and boiled before separation by sucrose gradient, but instead stirred in PBS with a magnetic stir bar until smooth (Figure S3). The most pure fraction, estimated to be 90% pure, was used for all of the structural characterization. The purity was determined by densitometry and confirmed by taking the ratio of the absorbance reading at 192 nm (peptide bond) and the absorbance at 220 nm (tryptophan residues) as previously described.[6] This purification protocol is reported to contain no trace of amyloid β.[37]

Monitoring the Kinetics of Tau Fibrillization. Recombinant monomeric tau protein was diluted to 135 μg/mL in PBS and boiled for 5 min with 100 mM β-mercaptoethanol. It was then incubated at 37 °C in a 200 μL reaction volume with an appropriate inducer (30 μg/mL heparin, 10 μL of partially purified 1% brain homogenate, or both) and 40 μM Thioflavin T (ThT). A 3 mm glass bead was added to each well to increase agitation with shaking before each 5 min fluorescence time reading. Thioflavin T fluorescence was monitored over time with excitation and emission filters set to 444 and 485 nm, respectively, in a Spectramax plate reader.[39] Fluorescence readings were taken every 5 min, with agitation for 3 s before each reading.

Far-UV Circular Dichroism. After the fibrillization reaction or purification of tau from AD brain tissue, the tau aggregates were centrifuged at 100 000g for 1 h at room temperature, and the pellets containing aggregates were resuspended in PBS to a resulting concentration of 50 μg/mL. Spectra were recorded on a Jasco J-815 spectrometer with a 10 mm path length quartz cell (Precision Cells) and reflect the average of three spectra accumulations. CD spectra readings were taken every 1 nm, at a scanning speed of 20 nm/min.

Electron Microscopy. Fibrillized protein was adsorbed onto glow-discharged carbon copper grids for 1 min (300 mesh, Electron Microscopy Sciences). After two successive 1 min washes with deionized water, each sample was negatively stained with 5% phosphotungstic acid (PTA) for 20 s. The grids were then observed on a Tecnai G2 12 Twin transmission electron microscope. Image analysis was done with ImageJ. The width of each fibril was measured every 20 nm with the scaled line selection drawing tool.[40] The periodicity measurement was taken with the same technique in ImageJ by measuring the distance between each complete twist that was available in every imaged fibril. The available number (n) of measurements for each fibril characteristic represents all of the measurements taken across biological and technical replicates. All fibril images were chosen from a random area on the EM grid to eliminate observer bias. Representative AD PHF EM images for each brain sample are shown in (Figure S4). Since the brain preparations from different tissue samples were relatively homogeneous and not statistically different from each other
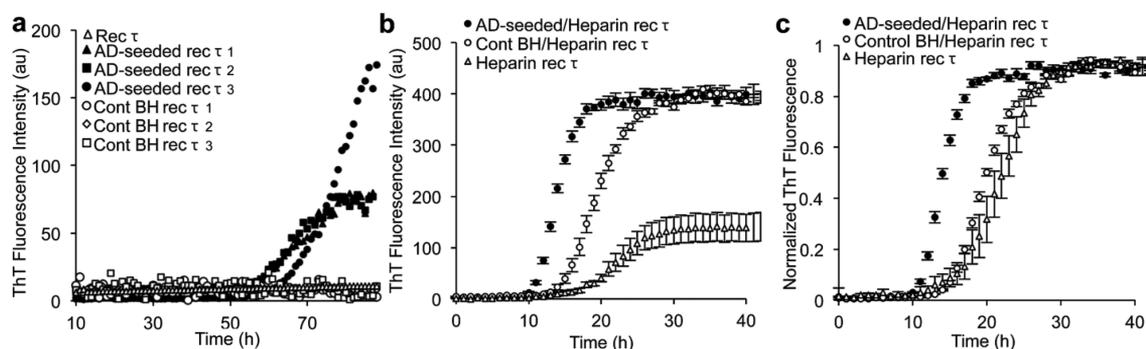
Figure 1. Misfolded tau in AD brain homogenate seeds the conversion of monomeric recombinant tau into amyloid. Tau fibrillization kinetics were monitored with Thioflavin T fluorescence. (a) Rec tau did not spontaneously form fibrils (open triangles). Misfolded tau isolated from AD brain homogenate (BH) samples induced rec tau fibrillization (black triangles, squares, circles), while comparable tau isolated from control BH did not (open circles, diamonds, squares). (b) Tau fibrillization kinetics in the presence of the polyanion heparin. Heparin induced tau fibrillization with a nucleation lag phase of 12.0 ± 0.8 h (open triangles). AD BH seeded the fibrillization reaction with a reduction in the lag phase to 8.8 ± 0.2 h (black circles), while a mock isolate of the control BH did not seed the reaction and retains the nucleation lag phase at 12.2 ± 0.8 h (open circles), though the total ThT fluorescence increased. (c) Normalized tau fibrillization kinetics from panel (b). The data points were normalized by subtracting background and dividing by the average value of the plateau observed at late time points.

in width and periodicity measurements, quantified image data for each sample type were pooled.

Denaturation and Quantification of Aggregated Tau. To quantify aggregated tau, reaction products are filtered through a membrane that traps and retains large protein aggregates (>0.2 μm), while small species, including protein monomers, pass through. The smaller species are bound to a nitrocellulose membrane, layered underneath the cellulose acetate filter membrane. Fibrillized protein was buffer exchanged into PBS by centrifugation at $100\,000g$ for 1 h and then resuspended to a final concentration of ~50 μg/mL in PBS. 30 μL of the protein solution was incubated in a titration of GdnHCl concentrations for 24 h. The protein solution was run on a Bio-Dot microfiltration apparatus through a cellulose acetate filter and nitrocellulose membrane. The membranes were developed with a 1:100 dilution of the N-terminal tau antibody 5A6 (Iowa Hybridoma Bank) and a mouse secondary HRP antibody (Invitrogen). Protein content was detected with chemiluminescence.

To compute the denaturation curves, chemiluminescence intensity at each protein-enriched dot was quantified with ImageJ, subtracting the background immediately outside of each measurement. The area of measurement was kept constant across each sample. Each denaturation curve was initially fit to a Hill equation using the MATLAB fitting tool, and then normalized to the highest y value of the fit.

■ RESULTS

Tau fibrils from 3 AD frontal cortex samples were partially purified using ultracentrifugation with sucrose cushions as previously described,[38] resulting in preparations of ~90% pure tau. Incubation of rec tau in the presence of the brain-derived fibrils induced tau fibrillization, as monitored by Thioflavin T (ThT) fluorescence (Figure 1a; filled symbols). In the absence of PHFs, rec tau did not spontaneously misfold (Figure 1a; open triangles). We prepared mock isolates from 3 normal human frontal cortex samples with the same purification procedure; additions of these control brain isolates to a solution of rec tau did not initiate a fibrillization reaction (Figure 1a; open symbols).

As expected,[15,32,33] incubation of rec tau with heparin-induced fibril formation (Figure 1b; open triangles), and

addition of PHFs to the reaction containing heparin accelerated fibril formation (Figure 1b-c, filled circles). The addition of the control fraction obtained from normal brain homogenate did not substantially reduce the nucleation lag phase, though the observed ThT signal increased (Figure 1b-c, open circles). The increase in the ThT signal at the plateau of the control brain heparin-induced reaction compared to the heparin-induced reaction may be due to impurities coeluted with the control brain fraction.

Tau fibrils isolated from AD brain tissue and those formed *in vitro* were characterized for differences in conformation. We used negative stain electron microscopy (EM) to compare the morphologies of the fibrils isolated from AD brain tissue (Figure 2a), AD-seeded rec tau fibrils (Figure 2b), and heparin-induced rec tau fibrils (Figure 2c). The resulting images were analyzed to quantify fibril width and twist periodicity. The AD brain tau and the AD-seeded rec tau structures formed *in vitro* shared comparable width (19.5 ± 0.4 nm vs 19.4 ± 0.4 nm) and periodicity (84.5 ± 1.0 nm vs 84.3 ± 1.0 nm), respectively. These values are consistent with previously reported observations of AD brain PHFs and straight filaments (SFs).[2,6] In contrast, the heparin-induced rec tau structures consisted of significantly ($p < 10^{-3}$) thinner 16.9 ± 0.3 nm tightly coiled rods and loose ribbons with a higher ($p < 10^{-3}$) periodicity of 129 ± 7 nm (Figure 2d-e).

We used circular dichroism (CD) spectroscopy to gain insight into differences in secondary structure[6,41] between fibril preparations (Figure 3). The AD brain PHFs and AD-seeded rec tau fibrils had similar CD spectra, with minima at 224 ± 1 nm and 225 ± 1 nm, respectively, while heparin-induced fibrils had a minimum at 209 ± 1 nm. To ensure that the spectra observed for AD-seeded rec tau fibers was due to fibrils formed during the seeding reaction and not simply those carried over from the AD brain derived seed itself, we measured the CD spectra of the AD brain-derived seed at seeding reaction concentration, and the resulting spectra was within the buffer noise (Figure S5).

Denaturants such as GdnHCl often solubilize aggregated proteins, with the concentration of GdnHCl required to achieve solubility reflecting the stability of the aggregate. Densitometric analysis of tau protein retained by a membrane with pore size of 0.2 μm following 24 h exposure to GdnHCl was used to assess
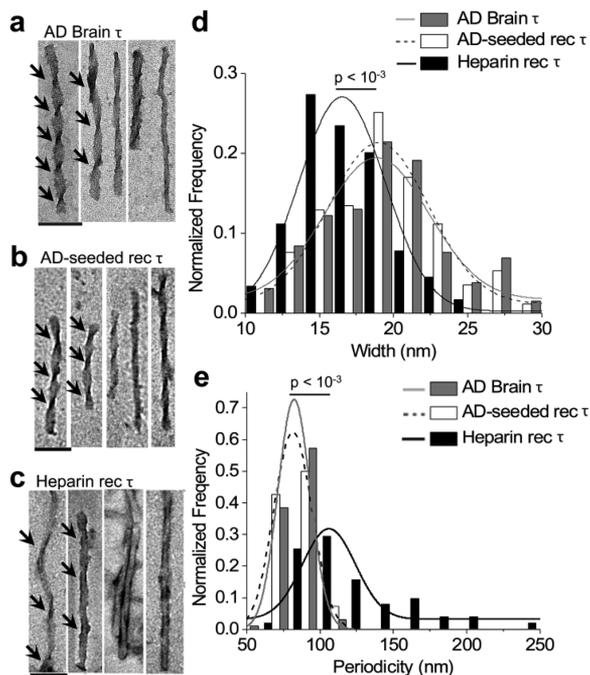
Figure 2. Fiber width and twist periodicity are conserved upon amyloid seeding. Electron microscopy was used to analyze the morphology of tau fibrils. Tau fibrils isolated from AD brain (a) were composed of a mixture of paired helical filaments and straight, untwisted filaments. AD-seeded rec tau fibrils (b) had a similar morphology to the disease-related form, while heparin-induced fibrils (c) were composed of mixture of tightly bound clusters of fibrils and twisted ribbons, with a higher length of periodicity. (d) Distributions of fibril width observed ($n > 100$). The average width of the AD brain tau fibers (gray bars), 19.4 ± 0.4 nm, was not statistically different from the average width of AD-seeded rec tau fibrils (white bars), 19.2 ± 0.4 nm. However, the average width of heparin-induced rec tau fibrils (black bars), 16.9 ± 0.3 nm, was significantly ($p < 10^{-3}$) thinner than the AD-isolated tau fibrils ($n > 50$). (e) The average periodicity of AD brain tau (gray bars) was 83.2 ± 1.0 nm. It was not statistically different from the average periodicity of AD-seeded rec tau fibrils (white bars), which was 84.5 ± 1.6 nm. The heparin-induced rec tau fibrils (black bars) had an average periodicity of 129.2 ± 7.1 nm, which was significantly ($p < 10^{-3}$) different from the AD-isolated tau fibrils. $n > 50$ for all distributions in (e). The scale bar in (a-c) represents 100 nm. The error in the reported means above denotes standard error.

the degree of unfolding of the aggregates (Figure 4a). The AD-seeded rec tau structure was significantly less stable than the heparin-induced structure, and more closely resembled the stability of the PHFs purified from AD brain. The midpoint denaturation ($GdnHCl_{1/2}$) values for AD brain tau and AD-seeded rec tau and were found to be at 2.3 (95% confidence interval 1.9−2.6) M GdnHCl and at 2.3 (2.0−2.6) M GdnHCl, respectively, while the heparin-induced tau fibrils had a $GdnHCl_{1/2}$ value at 3.2 (2.6−3.8) M GdnHCl (Figure 4b), consistent with the similarities and differences observed by EM and CD. Additionally, in 6 M GdnHCl, the heparin-induced rec tau remained $47\% \pm 8\%$ insoluble, while the AD brain tau fibrils and AD seeded rec tau fibrils were significantly more unfolded, retaining only $13\% \pm 4\%$ and $22\% \pm 5\%$ insoluble content, respectively. The significantly higher stability observed for the heparin-induced rec tau fibrils may result from tau-heparin interaction in the fibers.[42,43]

The distinct structures formed in the initial fibrillization assay were further propagated in a secondary seeding reaction
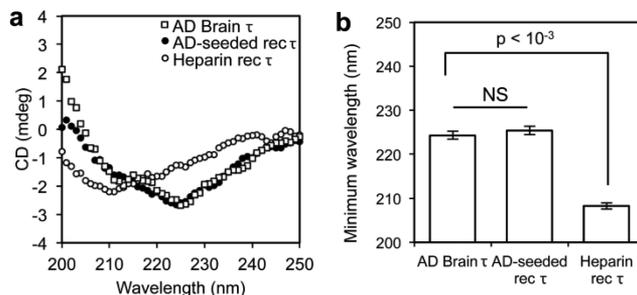
Figure 3. Analysis of fibril secondary structure by circular dichroism. (a) Representative CD spectra for AD Brain tau (open squares), AD-seeded rec tau (black circles), and heparin-induced rec tau fibril (open circles) conformations. (b) Quantification of the wavelength of minimum ellipticity in the CD curves. AD-seeded rec tau and AD brain tau fibrils did not significantly differ, having an average minimum peak in ellipticity at 225 ± 1 nm. Heparin-induced rec tau fibrils had a significantly lower ($p < 10^{-3}$) wavelength of minimum ellipticity, with an average minimum peak of 208 ± 1 nm. Error bars show standard error from 4 independent measurements of rec tau fibrils from different fibrillization assays and brain tissue samples.
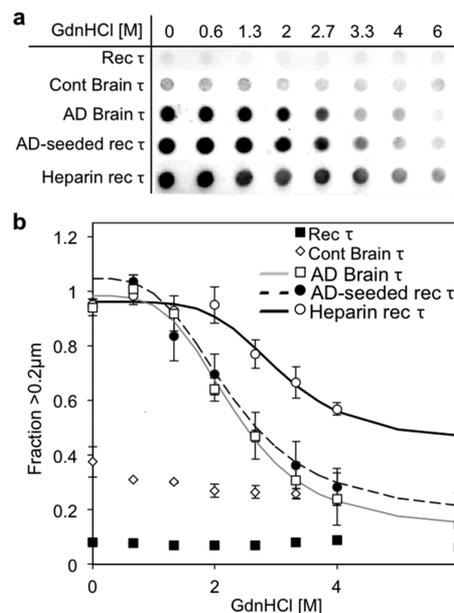
Figure 4. AD Brain tau and AD-seeded recombinant tau fibrils have similar stability with respect to GdnHCl denaturation. Solutions containing tau fibril preparations (AD Brain tau, AD-seeded rec tau, and heparin-induced rec tau) were incubated with varying GdnHCl concentrations for 24 h at room temperature. (a) Representative dot blot images of tau retained by the cellulose acetate membrane with 0.2 μm pores. (b) Quantified data from four independent experiments. The midpoint denaturation ($GdnHCl_{1/2}$) for AD brain tau (open squares) occurred at 2.3 M GdnHCl (95% confidence interval 2.0−2.6 M); AD-seeded rec tau fibrils (black circles) had a comparable $GdnHCl_{1/2}$ at 2.3 M (1.9−2.6) M; while heparin-induced rec tau fibrils (open circles) had a significantly higher $GdnHCl_{1/2}$ at 3.2 M (2.6−3.8) M. Note also that 47% of the heparin-induced fibrils remained >0.2 μm even after incubation with 6 M GdnHCl, while only 22% of the other fiber types remained insoluble ($p = 0.05$). Error bars denote standard error from measurements of rec tau fibrils from independent fibrillization assays and independent brain tissue samples.

(Figure 5). We incubated both the rec tau fibrils formed by AD brain PHF seeding and those formed by induction with heparin with fresh rec tau at 37 °C, with no additional heparin present.
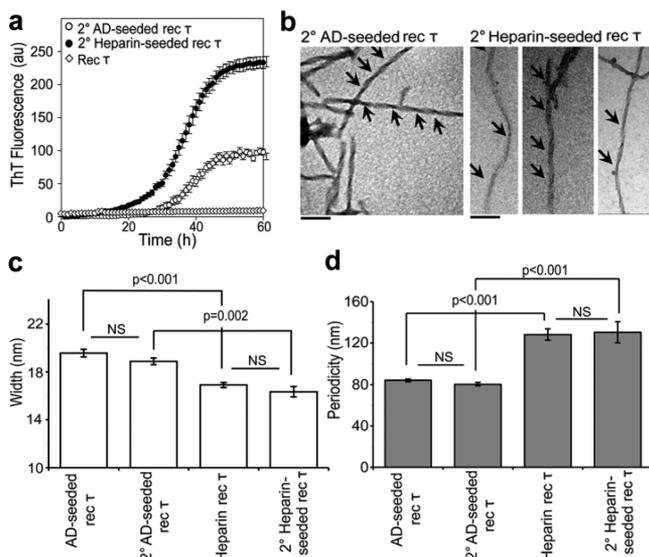
Figure 5. The distinct structures of AD-seeded rec τ fibrils and heparin rec τ fibrils are propagated through secondary seeding in solutions lacking heparin. Monomeric rec tau was incubated in the presence of a seed fibrillized in a previous *in vitro* reaction, and tau fibrillization was monitored with Thioflavin T fluorescence. (a) Characteristic curves of secondary tau fibrillization reactions using primary AD-seeded rec τ (black circles) fibrils and primary heparin rec tau (open circles) fibrils as seeds. (b) Representative electron microscopy figures of propagated AD tau fibril structures (left) and heparin rec tau fibril structures (right) with secondary seeding. The scale bar represents 100 nm. (c) Average width is preserved with seeding, $n > 100$. The secondary AD-seeded and heparin fibril seeded rec tau fibril widths (18.8 ± 0.3 nm and 16.3 ± 0.4 nm) are not significantly different from the primary AD-seeded and heparin-induced rec tau fibril widths (19.6 ± 0.4 nm and 16.9 ± 0.2 nm). (d) Average periodicity is also preserved with secondary seeding, $n > 15$. The secondary AD-seeded and heparin fibril seeded rec tau fibril periodicity (80.3 ± 1.6 nm and 128 ± 5 nm) is not significantly different from AD-seeded and heparin-induced rec tau fibril periodicity (84.0 ± 1.3 nm and 130 ± 10 nm).

The seed came directly from the primary reaction and accounted for 5% of the reaction volume. The fibrillization reaction kinetics were monitored with ThT fluorescence. The resulting fibril conformations were not statistically different from the seed conformations as determined by EM (Figure 5b). The secondary AD-seeded rec tau fibrils had a similar width (19.6 ± 0.4 nm vs 18.8 ± 0.3 nm) (Figure 5c) and periodicity (84.0 ± 1.3 nm vs 80.3 ± 1.6 nm) (Figure 5d) as those formed in the primary seeding reaction. Additionally, the secondary heparin fibril seeded rec tau fibrils had a similar width (16.3 ± 0.4 nm vs 16.9 ± 0.2 nm) (Figure 5c) and periodicity (130 ± 10 nm vs 128 ± 5 nm) (Figure 5d) compared to the primary heparin-induced seeds. The secondary AD-seeded rec tau fibril characteristics were significantly different ($p < 10^{-3}$) from the secondary heparin fibril seeded rec tau fibrils.

We also examined fibril structures formed in the presence of the heparin inducer, with and without the addition of PHFs and mock samples isolated from normal brain tissue (Figure 6). In electron micrographs, the resulting AD-seeded fibrils appeared to be a mixture of those observed for heparin-induced reactions and AD PHF seeded reactions. We observed an average width of 20.5 ± 0.2 nm (Figure 6b; black line) and a periodicity of 153 ± 2 nm (Figure 6c; gray line), and a general morphology of fibrils that were similar to both AD brain tau and heparin-induced rec tau fibrils. By EM, the mock seeded fibrils had
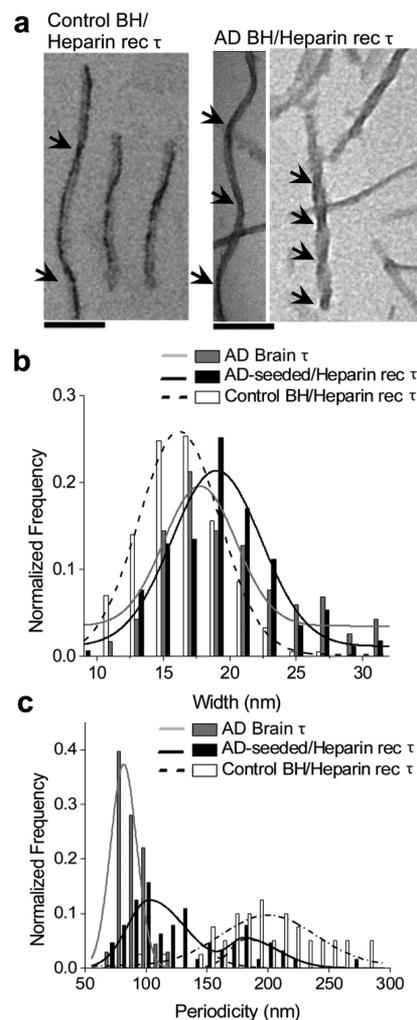
Figure 6. Addition of heparin corrupts the fidelity of AD PHF template propagation. (a) Representative electron micrographs of rec tau fibrils seeded with control (left) and AD brain tau isolated (right) in the presence of heparin. The average width of rec tau fibrils seeded with isolated AD brain tau fibrils in the presence of heparin (black bars) was 20.5 ± 0.3 nm, which was significantly ($p < 10^{-3}$) lower from the AD brain tau fibrils (gray bars), which have an average width of 19.4 ± 0.4 nm. Control brain tau isolates in the presence of heparin (white bars) induced a conformation of rec tau fibrils with an average width of 15.5 ± 0.3 nm. (c) Distributions of tau fibril periodicity ($n > 40$). In the presence of tau fibrils isolated from AD brain homogenate, the heparin-induced rec tau fibrils (black bars) had a heterogeneous population with an average periodicity of 221 ± 18 nm and were significantly ($p < 10^{-3}$) different from the AD brain tau fibrils (gray bars), which had a periodicity of 19.4 ± 0.4 nm. Control brain tau isolates (white bars) in the presence of heparin induced a rec tau fibril conformation with an average periodicity of 153 ± 2 nm. The scale bar represents 100 nm.

average width and periodicity of 15.5 ± 0.3 nm (Figure 6b; dashed line) and 221 ± 18 nm (Figure 6c; dashed line), respectively. CD analysis also supported the presence of distinct conformations in these fibrillization conditions (Figure S6). These results suggest that the presence of heparin corrupts the fidelity of PHF conformational propagation.

■ DISCUSSION

We hypothesized that the conformation of tau fibrils found in AD brain tissue may be propagated through conversion of

soluble recombinant tau into fibrils by a templating mechanism. We compared structural features of tau fibrils isolated from human AD brain samples to those formed *in vitro* with rec tau seeded with partially purified AD brain-derived PHFs, and also to those induced to fibrillize by incubation with heparin. Rec tau seeded with AD brain-derived PHFs formed a fibril conformation that shared fibril morphology, secondary structure and chemical stability with the AD brain-derived seed itself. In contrast, the heparin-induced fibril conformations were structurally distinct from the misfolded tau conformation found in AD brain. These distinct conformations were serially propagated in a secondary seeding reaction. Therefore, we propose that the seeded tau fibrillization process described here is an improved biochemical model of tau misfolding, because it preserves and propagates the original conformation of misfolded tau associated with AD. Our results also suggest that, *in vivo*, if PHFs infect nearby cells by a prion-like mechanism, they may seed normal tau to adopt their conformation, regardless of the initial phosphorylation state of tau in those neurons.

To purify rec tau for this study, we exploited the heat stability of tau by boiling the *E. coli* cell lysate for preliminary purification before ion-exchange. Alternate methods purify tau by precipitation with ammonium sulfate.[15] Boiling tau has been shown to result in the association of tau with heat-stable anionic impurities such as DNA.[44] It is possible that the fidelity of the structural propagation of tau relies on such cofactors.

While heparin-induced tau fibrils are a standard biochemical model for production of tau fibrils *in vitro*, previous structural characterization of heparin-induced full-length tau fibrils by electron microscopy have shown a heterogeneous population of structures with a different distribution of mass per length values than AD-isolated tau fibrils.[11,12] Tau fibrils isolated from AD brain are also found in two conformational populations of SFs and PHFs; however, these fibrils share a common structural unit.[45] In comparison, the heterogeneous heparin-induced rec tau conformations do not appear to be variations of the same underlying molecular conformation, as the mixture contains straight protofibrils which are thicker than the twisted ribbon fibrils present. Phosphorylated rec tau induced to fibrillize with heparin has been shown to have a more twisted, AD-like morphology,[15] but detailed structural analysis of such structures has not been reported. Additionally, during fibrillization, heparin binds to the fiber structure itself and stabilizes tau,[42,43,46] which may contribute to higher conformational stability of the fibrils formed.

Although previous work suggests that PHFs isolated from AD brain do not bind to or sequester normal tau into fibrils on a short time scale,[47] we find that after a prolonged incubation PHFs do seed the fibrillization of rec tau, demonstrating that tau does not have to be hyperphosphorylated to contribute to fibril growth. Although AD PHFs are primarily made up of abnormally phosphorylated tau even at the early stages of the disease,[3,7] these phosphorylation sites are localized to the amino- and carboxy-terminal flanking regions of the microtubule-binding domain,[48,49] which are accessible after tau assembly into PHFs. This suggests that aberrant tau seeds may sequester unmodified tau while propagating the disease-specific conformation, and become abnormally phosphorylated after fibril assembly. Recent evidence suggests that hyperphosphorylation of tau may be a protective response to the disease and may occur after tau fibrillization to defend the affected neurons and to escape from acute, stimulus-induced apoptosis.[10,50] The

sites of tau phosphorylation also change during neurofibrillary maturation.[51,52] Our findings suggest that although hyperphosphorylation may not be a direct consequence of tau misfolding, tau fibrils may grow by incorporating unphosphorylated tau protein that may later become differentially phosphorylated during the course of AD progression.

Here we have shown that nonphosphorylated recombinant 0N4R tau protein is sufficient for propagation of structural features of PHFs isolated from AD brain. Determining if other tau isoforms and phosphorylation states are competent in this regard may shed further light on the mechanism of tau filament propagation. The ability to assemble large quantities of tau filaments from rec tau protein in the presence of heparin has enabled high-resolution structural analysis of these fibrils, circumventing obstacles to the isolation of PHFs in sufficient yield and purity that would otherwise be required, as well as providing an opportunity to incorporate radioisotopic and other labels into the protein to probe its structure.[53] The biochemical model outlined in this work can make use of similar approaches while propagating the tau conformations found in disease brain. Generating these disease-associated fibril structures *in vitro* may also be useful for drug screening.

■ ASSOCIATED CONTENT

⑤ Supporting Information
Information on recombinant protein production (Figure S1) and the characterization of unfolded recombinant tau protein (Figure S2); a figure describing the isolation of tau from brain tissue (Figure S3); a figure with additional EM images of AD brain tau filaments and corresponding AD-seeded rec tau filaments (Figure S4); a figure with CD controls (Figure S5); and a figure with CD supporting structural characterization of tau fibrils from Figure 5 (Figure S6). This material is available free of charge via the Internet at http://pubs.acs.org.

■ AUTHOR INFORMATION

Corresponding Author
*E-mail colby@udel.edu; phone 302-831-3649.

Present Address
Anne Robinson, Department of Chemical and Biomolecular Engineering, Tulane University, New Orleans, LA 70118.

Notes
The authors declare no competing financial interest.

■ ACKNOWLEDGMENTS

■ REFERENCES

(1) Barghorn, S., Davies, P., and Mandelkow, E. (2004) Tau paired helical filaments from Alzheimer's disease brain and assembled in vitro are based on beta-structure in the core domain. *Biochemistry* 43, 1694–1703.

(2) Lee, V. M., Balin, B. J., Otvos, L., Jr., and Trojanowski, J. Q. (1991) A68: a major subunit of paired helical filaments and derivatized forms of normal Tau. *Science 251*, 675−678.

(3) Grundke-Iqbal, I., Iqbal, K., Tung, Y. C., Quinlan, M., Wisniewski, H. M., and Binder, L. I. (1986) Abnormal phosphorylation of the microtubule-associated protein tau (tau) in Alzheimer cytoskeletal pathology. *Proc. Natl. Acad. Sci. U.S.A. 83*, 4913−4917.

(4) Spillantini, M. G., Murrell, J. R., Goedert, M., Farlow, M. R., Klug, A., and Ghetti, B. (1998) Mutation in the tau gene in familial multiple system tauopathy with presenile dementia. *Proc. Natl. Acad. Sci. U.S.A. 95*, 7737−7741.

(5) Buee, L., Bussiere, T., Buee-Scherrer, V., Delacourte, A., and Hof, P. R. (2000) Tau protein isoforms, phosphorylation and role in neurodegenerative disorders. *Brain Res. Brain Res. Rev. 33*, 95−130.

(6) Sadqi, M., Hernandez, F., Pan, U., Perez, M., Schaeberle, M. D., Avila, J., and Munoz, V. (2002) Alpha-helix structure in Alzheimer's disease aggregates of tau-protein. *Biochemistry 41*, 7150−7155.

(7) Bancher, C., Brunner, C., Lassmann, H., Budka, H., Jellinger, K., Wiche, G., Seitelberger, F., Grundke-Iqbal, I., Iqbal, K., and Wisniewski, H. M. (1989) Accumulation of abnormally phosphory-lated tau precedes the formation of neurofibrillary tangles in Alzheimer's disease. *Brain Res. 477*, 90−99.

(8) Alonso, A., Zaidi, T., Novak, M., Grundke-Iqbal, I., and Iqbal, K. (2001) Hyperphosphorylation induces self-assembly of tau into tangles of paired helical filaments/straight filaments. *Proc. Natl. Acad. Sci. U.S.A. 98*, 6923−6928.

(9) Alonso, A. C., Grundke-Iqbal, I., and Iqbal, K. (1996) Alzheimer's disease hyperphosphorylated tau sequesters normal tau into tangles of filaments and disassembles microtubules. *Nat. Med. 2*, 783−787.

(10) Santacruz, K., Lewis, J., Spires, T., Paulson, J., Kotilinek, L., Ingelsson, M., Guimaraes, A., DeTure, M., Ramsden, M., McGowan, E., Forster, C., Yue, M., Orne, J., Janus, C., Mariash, A., Kuskowski, M., Hyman, B., Hutton, M., and Ashe, K. H. (2005) Tau suppression in a neurodegenerative mouse model improves memory function. *Science 309*, 476−481.

(11) von Bergen, M., Barghorn, S., Muller, S. A., Pickhardt, M., Biernat, J., Mandelkow, E. M., Davies, P., Aebi, U., and Mandelkow, E. (2006) The core of tau-paired helical filaments studied by scanning transmission electron microscopy and limited proteolysis. *Biochemistry 45*, 6446−6457.

(12) Xu, S., Brunden, K. R., Trojanowski, J. Q., and Lee, V. M. (2010) Characterization of tau fibrillization in vitro. *Alzheimers Dement. 6*, 110−117.

(13) Ramachandran, G., and Udgaonkar, J. B. (2011) Understanding the kinetic roles of the inducer heparin and of rod-like protofibrils during amyloid fibril formation by Tau protein. *J. Biol. Chem. 286*, 38948−38959.

(14) Barghorn, S., and Mandelkow, E. . (2002) Toward a unified scheme for the aggregation into Alzheimer paired helical filaments. *Biochemistry 41*, 11.

(15) Goedert, M., Jakes, R., Spillantini, M. G., Hasegawa, M., Smith, M. J., and Crowther, R. A. (1996) Assembly of microtubule-associated protein tau into Alzheimer-like filaments induced by sulphated glycosaminoglycans. *Nature 383*, 550−553.

(16) Frost, B., Ollesch, J., Wille, H., and Diamond, M. I. (2009) Conformational diversity of wild-type Tau fibrils specified by templated conformation change. *J. Biol. Chem. 284*, 3546−3551.

(17) Petkova, A. T., Leapman, R. D., Guo, Z., Yau, W. M., Mattson, M. P., and Tycko, R. (2005) Self-propagating, molecular-level polymorphism in Alzheimer's beta-amyloid fibrils. *Science 307*, 262−265.

(18) Kodali, R., and Wetzel, R. (2007) Polymorphism in the intermediates and products of amyloid assembly. *Curr. Opin. Struct. Biol. 17*, 48−57.

(19) Bessen, R. A., and Marsh, R. F. (1994) Distinct PrP properties suggest the molecular basis of strain variation in transmissible mink encephalopathy. *J. Virol. 68*, 7859−7868.

(20) Telling, G. C., Parchi, P., DeArmond, S. J., Cortelli, P., Montagna, P., Gabizon, R., Mastrianni, J., Lugaresi, E., Gambetti, P., and Prusiner, S. B. (1996) Evidence for the conformation of the pathologic isoform of the prion protein enciphering and propagating prion diversity. *Science 274*, 2079−2082.

(21) Colby, D. W., Giles, K., Legname, G., Wille, H., Baskakov, I. V., DeArmond, S. J., and Prusiner, S. B. (2009) Design and construction of diverse mammalian prion strains. *Proc. Natl. Acad. Sci. U.S.A. 106*, 20417−20422.

(22) Cobb, N. J., and Surewicz, W. K. (2009) Prion diseases and their biochemical mechanisms. *Biochemistry 48*, 2574−2585.

(23) Tanaka, M., Chien, P., Naber, N., Cooke, R., and Weissman, J. S. (2004) Conformational variations in an infectious protein determine prion strain differences. *Nature 428*, 323−328.

(24) Tessier, P. M., and Lindquist, S. (2009) Unraveling infectious structures, strain variants and species barriers for the yeast prion [PSI+]. *Nat. Struct. Mol. Biol. 16*, 598−605.

(25) Frost, B., Jacks, R. L., and Diamond, M. I. (2009) Propagation of tau misfolding from the outside to the inside of a cell. *J. Biol. Chem. 284*, 12845−12852.

(26) Guo, J. L., and Lee, V. M. (2011) Seeding of normal Tau by pathological Tau conformers drives pathogenesis of Alzheimer-like tangles. *J. Biol. Chem. 286*, 15317−15331.

(27) Guo, J. L., and Lee, V. M. (2013) Neurofibrillary tangle-like tau pathology induced by synthetic tau fibrils in primary neurons over-expressing mutant tau. *FEBS Lett. 587*, 717−723.

(28) Clavaguera, F., Bolmont, T., Crowther, R. A., Abramowski, D., Frank, S., Probst, A., Fraser, G., Stalder, A. K., Beibel, M., Staufenbiel, M., Jucker, M., Goedert, M., and Tolnay, M. (2009) Transmission and spreading of tauopathy in transgenic mouse brain. *Nat. Cell Biol. 11*, 909−913.

(29) Reyes, J. F., Rey, N. L., and Angot, E. (2013) Transmission of tau pathology induced by synthetic preformed tau filaments. *J. Neurosci. 33*, 6707−6708.

(30) Guo, J. L., Covell, D. J., Daniels, J. P., Iba, M., Stieber, A., Zhang, B., Riddle, D. M., Kwong, L. K., Xu, Y., Trojanowski, J. Q., and Lee, V. M. (2013) Distinct alpha-synuclein strains differentially promote tau inclusions in neurons. *Cell 154*, 103−117.

(31) Clavaguera, F., Akatsu, H., Fraser, G., Crowther, R. A., Frank, S., Hench, J., Probst, A., Winkler, D. T., Reichwald, J., Staufenbiel, M., Ghetti, B., Goedert, M., and Tolnay, M. (2013) Brain homogenates from human tauopathies induce tau inclusions in mouse brain. *Proc. Natl. Acad. Sci. U.S.A. 110*, 9535−9540.

(32) King, M. E., Ahuja, V., Binder, L. I., and Kuret, J. (1999) Ligand-dependent tau filament formation: implications for Alzheimer's disease progression. *Biochemistry 38*, 14851−14859.

(33) Friedhoff, P., von Bergen, M., Mandelkow, E. M., Davies, P., and Mandelkow, E. (1998) A nucleated assembly mechanism of Alzheimer paired helical filaments. *Proc. Natl. Acad. Sci. U.S.A. 95*, 15712−15717.

(34) Goedert, M., Spillantini, M. G., Cairns, N. J., and Crowther, R. A. (1992) Tau proteins of Alzheimer paired helical filaments: abnormal phosphorylation of all six brain isoforms. *Neuron 8*, 159−168.

(35) Brion, J. P., Hanger, D. P., Couck, A. M., and Anderton, B. H. (1991) A68 proteins in Alzheimer's disease are composed of several tau isoforms in a phosphorylated state which affects their electro-phoretic mobilities. *Biochem. J. 279* (Pt 3), 831−836.

(36) Levy, S. F., Leboeuf, A. C., Massie, M. R., Jordan, M. A., Wilson, L., and Feinstein, S. C. (2005) Three- and four-repeat tau regulate the dynamic instability of two distinct microtubule subpopulations in qualitatively different manners. Implications for neurodegeneration. *J. Biol. Chem. 280*, 13520−13528.

(37) Greenberg, S. G., and Davies, P. (1990) A preparation of Alzheimer paired helical filaments that displays distinct tau proteins by polyacrylamide gel electrophoresis. *Proc. Natl. Acad. Sci. U.S.A. 87*, 5827−5831.

(38) Lee, V. M., Wang, J., and Trojanowski, J. Q. (1999) Purification of paired helical filament tau and normal tau from human brain tissue. *Methods Enzymol. 309*, 81−89.

(39) Rogers, D. R. (1965) Screening for Amyloid with the Thioflavin-T Fluorescent Method. *Am. J. Clin. Pathol. 44*, 59−61.

(40) Gras, S. L., Waddington, L. J., and Goldie, K. N. (2011) Transmission electron microscopy of amyloid fibrils. *Methods Mol. Biol. 752*, 197−214.

(41) Chen, Y. H., Yang, J. T., and Martinez, H. M. (1972) Determination of the secondary structures of proteins by circular dichroism and optical rotatory dispersion. *Biochemistry 11*, 4120−4131.

(42) Zhu, H. L., Fernandez, C., Fan, J. B., Shewmaker, F., Chen, J., Minton, A. P., and Liang, Y. (2010) Quantitative characterization of heparin binding to Tau protein: implication for inducer-mediated Tau filament formation. *J. Biol. Chem. 285*, 3592−3599.

(43) Sibille, N., Sillen, A., Leroy, A., Wieruszeski, J. M., Mulloy, B., Landrieu, I., and Lippens, G. (2006) Structural impact of heparin binding to full-length Tau as studied by NMR spectroscopy. *Biochemistry 45*, 12560−12572.

(44) Kar, S., Fan, J., Smith, M. J., Goedert, M., and Amos, L. A. (2003) Repeat motifs of tau bind to the insides of microtubules in the absence of taxol. *EMBO J. 22*, 70−77.

(45) Crowther, R. A. (1991) Straight and paired helical filaments in Alzheimer disease have a common structural unit. *Proc. Natl. Acad. Sci. U.S.A. 88*, 2288−2292.

(46) Hasegawa, M., Crowther, R. A., Jakes, R., and Goedert, M. (1997) Alzheimer-like Changes in Microtubule-associated Protein Tau Induced by Sulfated Glycosaminoglycans. *J. Biol. Chem. 272*, 6.

(47) Alonso Adel, C., Li, B., Grundke-Iqbal, I., and Iqbal, K. (2006) Polymerization of hyperphosphorylated tau into filaments eliminates its inhibitory activity. *Proc. Natl. Acad. Sci. U.S.A. 103*, 8864−8869.

(48) Hanger, D. P., Betts, J. C., Loviny, T. L., Blackstock, W. P., and Anderton, B. H. (1998) New phosphorylation sites identified in hyperphosphorylated tau (paired helical filament-tau) from Alzheimer's disease brain using nanoelectrospray mass spectrometry. *J. Neurochem. 71*, 2465−2476.

(49) Cripps, D., Thomas, S. N., Jeng, Y., Yang, F., Davies, P., and Yang, A. J. (2006) Alzheimer disease-specific conformation of hyperphosphorylated paired helical filament-Tau is polyubiquitinated through Lys-48, Lys-11, and Lys-6 ubiquitin conjugation. *J. Biol. Chem. 281*, 10825−10838.

(50) Li, H. L., Wang, H. H., Liu, S. J., Deng, Y. Q., Zhang, Y. J., Tian, Q., Wang, X. C., Chen, X. Q., Yang, Y., Zhang, J. Y., Wang, Q., Xu, H., Liao, F. F., and Wang, J. Z. (2007) Phosphorylation of tau antagonizes apoptosis by stabilizing beta-catenin, a mechanism involved in Alzheimer's neurodegeneration. *Proc. Natl. Acad. Sci. U.S.A. 104*, 3591−3596.

(51) Lasagna-Reeves, C. A., Castillo-Carranza, D. L., Sengupta, U., Sarmiento, J., Troncoso, J., Jackson, G. R., and Kayed, R. (2012) Identification of oligomers at early stages of tau aggregation in Alzheimer's disease. *FASEB J 26*, 1946−1959.

(52) Kimura, T., Ono, T., Takamatsu, J., Yamamoto, H., Ikegami, K., Kondo, A., Hasegawa, M., Ihara, Y., Miyamoto, E., and Miyakawa, T. (1996) Sequential changes of tau-site-specific phosphorylation during development of paired helical filaments. *Dementia 7*, 177−181.

(53) Daebel, V., Chinnathambi, S., Biernat, J., Schwalbe, M., Habenstein, B., Loquet, A., Akoury, E., Tepper, K., Muller, H., Baldus, M., Griesinger, C., Zweckstetter, M., Mandelkow, E., Vijayan, V., and Lange, A. (2012) beta-Sheet core of tau paired helical filaments revealed by solid-state NMR. *J. Am. Chem. Soc. 134*, 13982−13989.